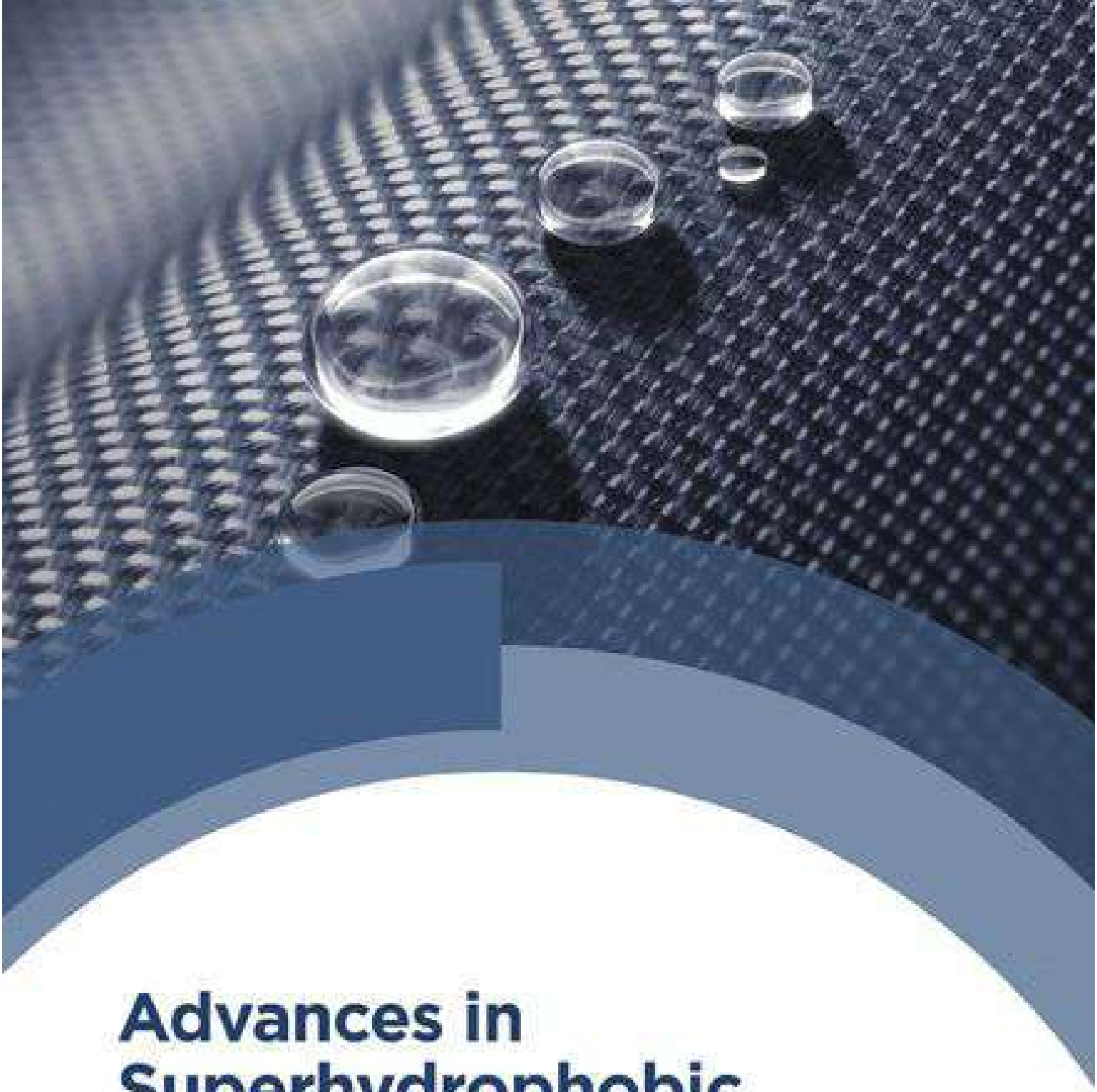

Advances in Superhydrophobic Coatings

Edited by Viswanathan S. Saji

ROYAL SOCIETY OF CHEMISTRY

Contents

Advances in Superhydrophobic Coatings
Edited by Viswanathan S. Saji

Published by the Royal Society of Chemistry, www.rsc.org

CHAPTER 16

Superhydrophobic Coatings for Oil–Water Separation

SANJAY S. LATTHE (0000-0002-6349-666X)*[a], PRADIP P. GAIKWAD[b], AKSHAY R. JUNDLE[b], SAGAR S. INGOLE[b], RAJARAM S. SUTAR[b], KISHOR KUMAR SADASIVUNI[c] AND SHANHU LIU (0000-0003-1382-7157)*[d]

[a]Self-cleaning Research Laboratory, Department of Physics, Vivekanand College (Autonomous), (Affiliated to Shivaji University, Kolhapur), Kolhapur 416003, Maharashtra, India; [b]Self-cleaning Research Laboratory, Department of Physics, Raje Ramrao Mahavidyalaya, (Affiliated to Shivaji University, Kolhapur), Jath, Sangli 416404, Maharashtra, India; [c]Center for Advanced Materials, Qatar University, P.O. Box 2713, Doha, Qatar; [d]Henan Key Laboratory of Polyoxometalate Chemistry, Henan Joint International Research Laboratory of Environmental Pollution Control Materials, College of Chemistry and Chemical Engineering, Henan University, Kaifeng 475004, China
*E-mail: latthes@gmail.com, liushanhu@vip.henu.edu.cn

16.1 Introduction

Frequent oil spills in the ocean and the dumping of oily wastes from industry into water bodies pose serious environmental problems. The critical challenge is to remove oil from the oil-contaminated water. Therefore, advanced technologies are essential to separate oil and water from oil–water mixtures. Expensive and time-consuming traditional methods have been used to retreat oily wastewater.[1] Recently, much effort has been expended on the efficient use of functional materials for the modification of porous substrates

Advances in Superhydrophobic Coatings
Edited by Viswanathan S. Saji

Published by the Royal Society of Chemistry, www.rsc.org

that can strongly repel water and easily absorb oil or penetrate into it, so that oil can be easily removed from mixtures of oil and water. This property of the surface is referred to as superhydrophobic [water contact angle (WCA) > 150°] and superoleophilic [oil contact angle (OCA) ~ 0°]. Considering this advanced surface feature, attempts have been made to fabricate superhydrophobic/superoleophilic meshes, cotton fabrics, membranes and sponges by depositing functional materials for effective oil–water separation (Figure 16.1).[2] For the efficient separation of oil from water, the material must exhibit a high absorption capability towards different oils and organic liquids, high separation efficiency and high reusability along with high mechanical, thermal and chemical sustainability under harsh conditions. Surface wettability is influenced by the surface topography and the presence of low surface energy chemical groups on the surface. In the Cassie–Baxter model, the surface

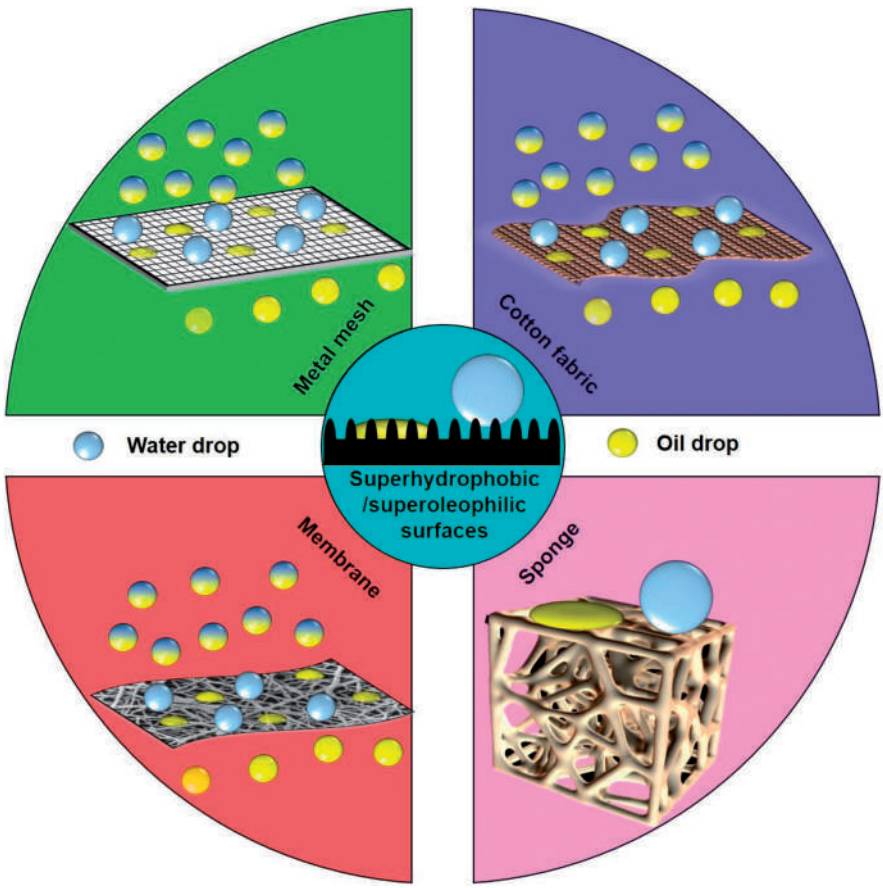

Figure 16.1 Schematic diagram of oil–water separation using superhydrophobic/superoleophilic mesh, cotton fabric, sponge and membrane.

roughness factor is an essential element in controlling wettability.[3] Along with low surface energy molecules, the hydrophobicity of rough surfaces can be significantly improved. Currently, superhydrophobic surfaces are fabricated by forming rough structures on hydrophobic materials or reducing the surface energy of rough surfaces by chemical modification.[4,5]

This chapter describes various techniques developed for the fabrication of superhydrophobic/superoleophilic surfaces and processes for the separation of oil–water mixtures using superhydrophobic/superoleophilic substrates. Attention is particularly focused on substrates such as metal meshes, cotton fabrics, membranes and sponges that have given promising results in the separation of oil from oil–water mixtures.

16.2 Fabrication Techniques for Superhydrophobic Coatings

Studies on the superhydrophobic phenomena of natural surfaces (plant leaves and animal/insect skin) have indicated that two important factors, surface topography and the presence of low surface energy chemical groups on the surface, are required for the fabrication of superhydrophobic coatings, and to achieve such superhydrophobic surfaces various techniques can be used in practice (Figure 16.2). The common techniques described in the following subsections are electrospinning,[6] the sol–gel technique,[7] the layer-by-layer method,[8] dip coating,[9] spray coating[10] and electrodeposition.[11]

16.2.1 Electrospinning

Electrospinning is a versatile and effective technique for producing highly porous and flexible micro- and nanosized fibre membranes.[12] During the electrospinning process, a high electric field (5–30 kV) is applied between the syringe needle and the collector, resulting in conversion of liquid drops into a jet and forming fine fibres by the effect of stretching and elongation of the jet. The liquid is forced out of the needle by the surface tension of the liquid drop, becoming a pendant droplet. When a droplet is sufficiently charged, electrostatic repulsion changes its shape and produces a Taylor cone, resulting in a polarized jet. The jet first goes in straight and then becomes deposited on the collector. The jet has a small diameter, so it quickly solidifies and deposits as a solid fibre on the collector.[13] In the synthesis of a polymer membrane, the diameter of the fibre and the porosity of the membrane are dependent on the solution flow rate, applied voltage, drum revolutions per minute (rpm), molecular weight of the polymer, solution viscosity, needle diameter and needle tip to collector distance. The resulting polymer membrane is mostly hydrophobic, and surface modification is necessary for superhydrophobicity.[14,15] A schematic diagram of electrospinning is shown in Figure 16.2a.

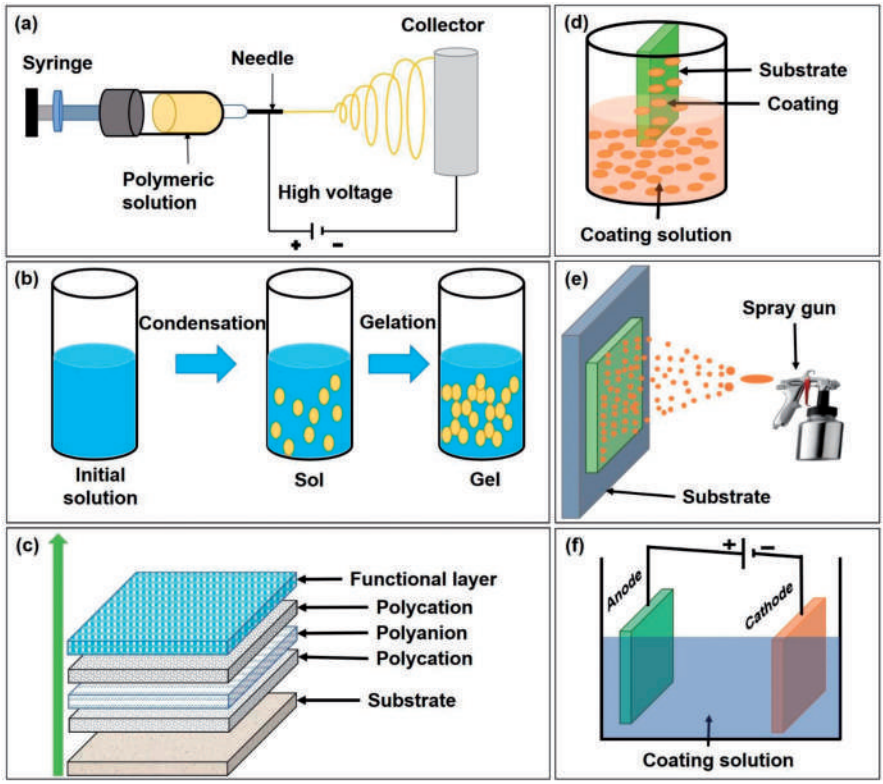

Figure 16.2 Schematic diagrams of (a) electrospinning, (b) sol–gel, (c) layer-by-layer, (d) dip-coating, (e) spray-coating and (f) electrodeposition techniques.

16.2.2 Sol–Gel Technique

The sol–gel technique is a simple, low-cost, widely accepted, rapid, low-temperature and eco-friendly method for producing a wide range of nano-structured coatings/films. It is the most preferred approach for obtaining good-quality coatings with controlled thickness. The method involves five processing steps: sol preparation, hydrolysis, condensation, growth of particles and agglomeration.[16] The sol–gel processed materials can be deposited on the substrate by dip-, spin- and spray-coating methods. Tetraethyl orthosilicate (TEOS) and tetramethyl orthosilicate (TMOS) are the most commonly used silicon alkoxides for the synthesis of silica-based materials by the sol–gel technique.[17] A schematic diagram of the sol–gel process is shown in Figure 16.2b.

16.2.3 Layer-by-Layer Method

The layer-by-layer deposition method is a preferred approach to produce hierarchical superhydrophobic coatings by controlling the coating thickness. Deposition occurs by repeated application of molecular monolayers on

the substrate surface through electrostatic interactions between the layers. The layer-by-layer deposition can be done using immersion, spraying and electrodeposition methods.[18] Multiple deposited layers produce large-scale roughness on the substrate surface and post-modification of the surface is required to obtain superhydrophobicity.[19,20] A schematic diagram of the layer-by-layer technique is shown in Figure 16.2c.

16.2.4 Dip Coating

Dip coating is a widely used, simple and inexpensive technique for coating onto any solid substrate, including glass, fibrous surfaces, polymer films, metals and ceramics for various purposes.[21] A wet liquid film is formed on the substrate by vertical immersion of the substrate in the coating solution and vertical withdrawal at a constant speed. Good quality of the coating film can be obtained by controlling parameters such as the speed of immersion and withdrawal, dipping time, drainage and evaporation of the solvent.[22] Owing to the capillary effect, the coating solution adheres to the substrate surface and excess solution drains off. After evaporation of the solvent, a thin layer of coating is formed on the substrate.[23,24] More importantly, any shape of the substrate can be coated using the dip-coating technique. The viscosity, surface tension, density and pH of the coating solution and also humidity, number of immersion cycles and temperature can affect the quality of the coating.[25] A schematic diagram of the dip-coating technique is shown in Figure 16.2d.

16.2.5 Spray Coating

The spray-coating method is widely used for large-scale production, since there are no size restrictions for substrates.[26] The parameters used, including flow rate, air pressure, substrate temperature, solution concentration, spray time, co-solvent combination, distance between nozzle and substrate and number of spray cycles, impact the coating.[27] Spray coating is used for producing high-quality thin films on an industrial scale.[28] A schematic diagram of the spray-coating technique is shown in Figure 16.2e.

16.2.6 Electrodeposition

Electrodeposition is a flexible and popular deposition technique that uses a cell with a working electrode and a counter electrode to generate current at a pre-set voltage.[29] The working electrode is the substrate on which metal ions are deposited as a result of a chemical reaction controlled by an applied current or voltage. In this process, the substrate attains a different kind of surface topography. Sometimes, chemical modification is required to change the wetting properties of the surface.[30] A schematic diagram of electrodeposition is shown in Figure 16.2f.

16.3 Superhydrophobic Coatings for Oil–Water Separation

16.3.1 Superhydrophobic Meshes

Metal meshes are ductile, have high mechanical strength and have a porous structure that allows liquids to penetrate readily. Therefore, the use of metal meshes as a substrate has attracted considerable attention for application in oil–water separations with changes to their surface wetting properties. Zulfiqar *et al.* deposited naturally available biowaste sawdust particles in combination with polychloroprene adhesive, carbon soot and silicone polymer on a stainless-steel (SS) mesh for oil–water separation. The polychloroprene adhesive was first applied on the SS mesh with a metal strip, then sawdust particles were applied with the help of a brush and the substrate was dipped in silicone solution. Carbon soot particles were deposited on the substrate by holding it over a flame and then dipping it in silicone solution to obtain a highly superhydrophobic and mechanically stable coating. The coated superhydrophobic SS mesh showed an oil separation efficiency of >90% for *n*-hexane, chloroform, toluene and dichloromethane. The coated mesh maintained its separation efficiency for five separation cycles and retained its superhydrophobic properties after mechanical abrasion.[31] Chen *et al.* fabricated a superhydrophobic poly(ethylene terephthalate) (PET) mesh by dipping it in a solution of polydimethylsiloxane (PDMS) and fluorinated silica (F-SiO_2) for use in oil–water separation. In an investigation of the relation between oil–water separation efficiency and pore size of the mesh, they found that the pore size of the mesh had a significant impact on the oil–water separation ability. A smaller pore size resulted in a lower apparent surface energy of the superhydrophobic PET mesh.[32] Singh *et al.* prepared a superhydrophobic copper mesh for oil–water separation by a fabrication process involving the oxidation of the copper mesh followed by low-pressure annealing at low temperature; the latter treatment enhanced the hydrophobicity of the mesh by the formation of a Cu_2O surface layer. The copper mesh was partially oxidized by treating it with hydrogen peroxide (H_2O_2) solution and then immersed in anhydrous ethanol for reduction, and eventually the copper mesh became superhydrophobic in nature. The structural morphology of the copper mesh changed during the treatment, as shown in Figure 16.3a. The scanning electron microscope (SEM) image in Figure 16.3b demonstrates that the during the oxidation and reduction process, the copper mesh became rougher. The pristine copper mesh showed a WCA of 120° and after oxidation and reduction the mesh had WCA values of 57 and 153°, respectively. The superhydrophobic mesh showed a separation efficiency of >99% for an oil–water mixture containing *n*-hexane, *n*-octane, *n*-decane, *n*-hexadecane and liquid paraffin. Even after 40 cycles of separation of an *n*-hexadecane–water mixture the mesh maintained a 99% separation efficiency.[33]

Tudu and Kumar prepared superhydrophobic meshes (steel and copper) by dipping into a solution of a mixture of perfluorodecyltriethoxysilane

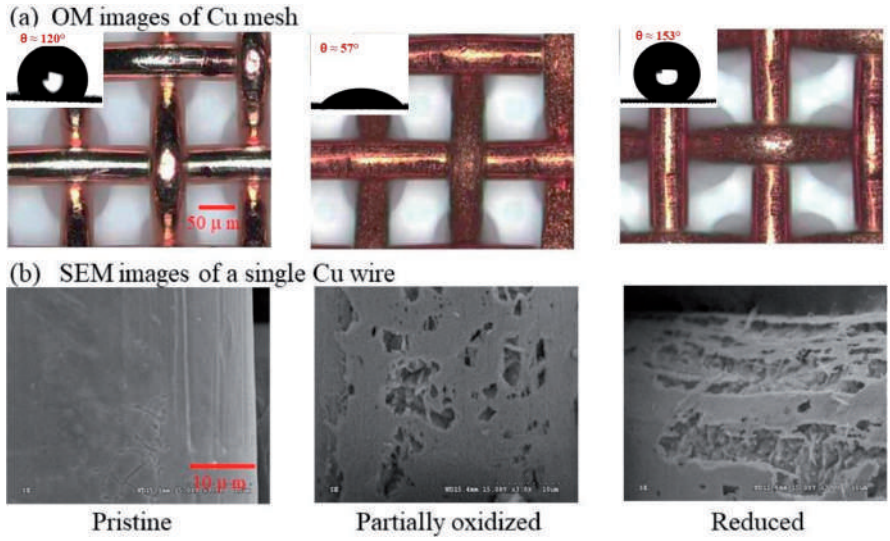

Figure 16.3 (a) Optical microscope (OM) images of pristine and treated (oxidation and reduction) copper meshes, the insets show the water drop images. (b) SEM images of single Cu wire pristine and treated (oxidation and reduction) copper meshes. Reproduced from ref. 33 with permission from Elsevier, Copyright 2018.

(PFDTS) and TiO_2 nanoparticles (NPs). The superhydrophobic steel and copper mesh surfaces obtained exhibited WCA values of 161 ± 2 and 159 ± 3°, respectively. The coated meshes retained their superhydrophobic properties even when exposed to extreme environmental conditions such as corrosive chemicals, high temperatures and mechanical disturbances and showed excellent self-cleaning ability. The copper mesh showed greater stability for oil–water (benzene and water) separations up to 100 cycles with a separation efficiency of 98%. The copper mesh separated oil-in-water (surfactant-free toluene-in-water) emulsions more efficiently than the steel mesh.[34] Varshney *et al.* synthesized a superhydrophobic/superoleophilic steel mesh using a chemical etching method. The mesh was immersed in mixture of hydrochloric acid and nitric acid, then washed with ethanol and distilled water and finally modified with lauric acid. The chemically modified mesh showed a WCA of 171 ± 4.5° and a separation efficiency of more than 99% for benzene–water and petroleum ether–water mixtures. The process for oil–water separation is shown in Figure 16.4.[35]

Comparative results of ongoing research on meshes are presented in Table 16.1.

16.3.2 Superhydrophobic Sponges

A 3D porous sponge facilitates high liquid absorption and is one of the superior substrates in the separation of oil–water mixtures. Cho *et al.* prepared a superhydrophobic nanocomposite film by dipping melamine sponge in a

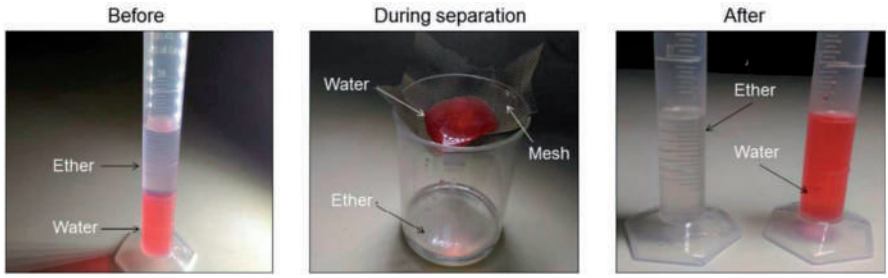

Figure 16.4 Experimental setup demonstrating the separation of petroleum ether and water. The water is coloured for ease of visualization. During separation, the ether penetrated through the coated mesh and water was retained on the coated mesh surface. Reproduced from ref. 35 with permission from the Royal Society of Chemistry.

blend of ormosil (organically modified silica) suspension and polymethylhydroxysiloxane followed by modification with perfluorooctyltriethoxysilane NPs to further improve the superhydrophobicity. The superhydrophobic sponge showed an absorption capacity of >80 g g^{-1} for chloroform and excellent recycling performance of up to 20 cycles against chloroform, pump oil and hexane.[36] Peng *et al.* applied a PDMS layer on a melamine sponge by the dip-coating technique followed by UV irradiation to obtain a superhydrophobic sponge. The PDMS-coated melamine sponge showed a WCA of 156.2°, and absorbed oil and organic solvents up to 103–179 times its own weight.[37]

Zou *et al.* fabricated superhydrophobic/superoleophilic high-density polyethylene (HDPE) aerogel-coated natural rubber latex foam (NRLF) for oil–water separation through a phase separation method. The HDPE aerogel-coated NRLF showed a porous structure and particle-like morphology with a WCA of >150°. The modified NRLF was an excellent absorbent against *n*-hexane and carbon tetrachloride.[38] Sun *et al.* prepared a superhydrophobic porous melamine sponge by immersion in lignin–hexadecyltrimethoxysilane (HDTMS) solution under sonication. The superhydrophobic melamine sponge showed a separation efficiency of >98.6% for different types of oil–water mixtures and excellent durability for 35 cycles of oil–water separation. The sponge showed a separation efficiency of >98.7% up to 100 cycles.[39] Liu *et al.* dip coated a sodium dodecylbenzene sulfonate-modified magnesium hydroxide particle suspension on melamine sponge. The coated sponge showed a WCA of 163 ± 3° and an OCA of 0°. The superhydrophobic/superoleophilic sponge exhibited excellent demulsification for immiscible oil–water mixtures, surfactant-free emulsions and surfactant-stabilized emulsions.[40]

Comparative results of ongoing research using sponges as substrates are given in Table 16.2.

Table 16.1 Representative reports on superhydrophobic/superoleophilic meshes for oil–water separation.

Materials	Mesh type	Method	Types of oil/organic solvent	WCA/°	Separation efficiency/%	Reusability/ cycles	Ref.
Sawdust, polychloroprene glue, RTV-1 silicone adhesive, paraffin wax candle	Steel	Dip coating	*n*-Hexane, toluene, chloroform, dichloromethane	155 ± 4	90	5	31
Silica NPs (20 nm), 1*H*,1*H*,2*H*,2*H*-perfluorodecyltriethoxysilane, polydimethylsiloxane, prepolymer	PET	Two-step impregnation	Trichloromethane, kerosene, octane, *n*-decane, *n*-hexane	155.9 ± 1.0	98 for kerosene	—	32
Sodium *n*-dodecyl sulfate, *n*-hexadecane, polystyrene, poly(vinyl acetate), polytetrafluoroethylene (PTFE)	Copper	Oxidation and casting	*n*-Hexane, *n*-hexadecane, *n*-octane, *n*-decane, liquid paraffin	~153	>99	40	33
Perfluorodecyltriethoxysilane (PFDTS), TiO_2 NPs	Steel and copper	Dip coating	Benzene	Copper mesh 159 ± 3 SS mesh 161 ± 2	99	Copper mesh 80 SS mesh 50	34
HNO_3, HCl, ethanol, lauric acid	Steel	Chemical etching (*not a coating method*)	Petroleum ether, benzene	171 ± 4.5	>99	10	35

Table 16.2 Representative reports on superhydrophobic/superoleophilic sponges for oil–water separation.

Materials	Sponge type	Method	Types of oil/organic solvent	WCA/°	Absorption capacity/g g^{-1}	Reusability/ cycles	Ref.
Methyltriethoxysilane, polymethylhydroxysiloxane, triethoxy(octyl)silane, hexadecyltrimethoxysilane, triethoxyphenylsilane(phenylsilane), 1*H*,1*H*,2*H*,2*H* perfluorooctyltriethoxysilane	Melamine	Immersion	Methanol, ethanol, dimethylformamide (DMF), *n*-hexane, dimethyl sulfoxide, chloroform, acetone, pump oil, tetrahydrofuran, motor oil	168	35–82	30	36
Polymethylvinylsilicone with a vinyl content of 10 mol, pentaerythritol tetrakis(2-mercaptoacetate)	Melamine	Dip coating	Machine oil, silicone oil, pump oil, used pump oil, diesel oil, soyabean oil, cyclohexane, acetone, chloroform, DMF, ethyl acetate	156.2	103–179	10	37
Natural rubber latex, high-density polyethylene	Latex	Thermally induced phase separation	Colza oil, silicone oil, *n*-hexane, toluene, carbon tetrachloride, acetone, chloroform, methanol	>150	5–7	40	38
Hardwood kraft lignin, hexadecyltrimethoxysilane	Melamine resin	Simple impregnation	Chloroform, *n*-hexane, petroleum ether, methylbenzene, peanut oil, kerosene	162 ± 1.2	40–100	35	39
Magnesium hydroxide hexahydrate, stearic acid, sodium dodecylbenzene sulfonate, sodium lauryl sulfate, cetyltrimethylammonium bromide, poly(acrylic acid)	Melamine	Immersion	Vacuum pump oil, dichloromethane, *n*-hexane, carbon tetrachloride, toluene, edible oil, petroleum ether	163 ± 3	77–145	50	40

16.3.3 Superhydrophobic Cotton Fabrics

Cheng *et al.* prepared a fluorine-free superhydrophobic cotton fabric *via* the enzyme etching method and coated its surface with epoxidized soybean oil and stearic acid. The coated cotton fabric sustained its superhydrophobic property against mechanical abrasion, tape peeling, ultrasonication, chemical resistance and low/high-temperature treatments. The superhydrophobic cotton fabric showed an oil–water separation efficiency of 98%.[41] Gao *et al.* prepared fabricated superhydrophobic coatings on 2D fabric and 3D sponge through a phase separation method. In this process, PDMS dissolved in tetrahydrofuran (THF) and water as a non-solvent was added for phase separation. The modified 2D or 3D porous substrates exhibited a good separation ability for various types of oil–water mixtures.[42] Li *et al.* deposited a suspension of copper stearate (CS) and PDMS on various substrates such as iron, paper, glass, copper and fabric *via* spraying, dipping and brushing for the preparation of superhydrophobic surfaces. Among them, CS/PDMS-coated cotton effectively separated oil–water mixtures and oil–water emulsions. The prepared fabric showed high water repellency and oil absorbance ability. The process for the separation of oil–water mixtures is shown in Figure 16.5a. An emulsion was prepared with water and toluene. During the oil–water separation, the toluene was easily removed from the emulsion, as shown in Figure 16.5b.[43]

Talebizadehsardari *et al.* deposited a superhydrophobic nanocomposite of PDMS/silica NPs on cotton fabric by a dip-coating method. The superhydrophobic cotton fabric showed an effective separation efficiency of 97–99% for paraffin oil, toluene, hexane and a vegetable oil–water mixture. With respect to reusability, the superhydrophobic cotton fabric showed a separation efficiency of 95% even after 50 separation cycles.[44] Dong *et al.* prepared

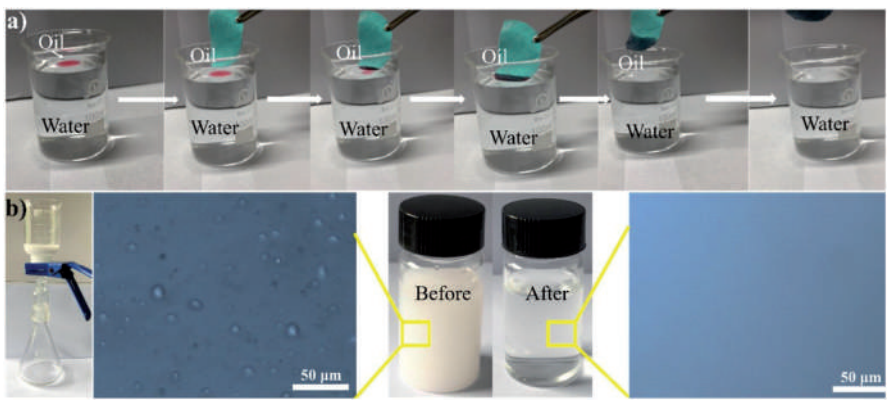

Figure 16.5 (a) Photograph of the oil–water separation process using the coated fabric. (b) Optical micrographs of the emulsion before and after separation. Reproduced from ref. 43 with permission from Elsevier, Copyright 2020.

Table 16.3 Representative reports on superhydrophobic/superoleophilic fabrics for oil–water separation.

Materials	Method	Types of oil/organic solvent	WCA/°	Separation efficiency/%	Reusability/ cycles	Ref.
Epoxidized soybean oil, 1,8-diazabicyclo[5.4.0]undec-7-ene, sebacic acid, stearic acid	Enzyme etching followed by surface coating and subsequent surface modification	Chloroform, toluene, cyclohexane, silicone oil, *n*-heptane, soybean oil, petroleum ether	157.3	98	10	41
Tetrahydrofuran, hexadecane, polydimethylsiloxane	Phase separation	Dichloromethane	155.0	~100	—	42
Polydimethylsiloxane, copper acetate, stearic acid	Dipping, spraying, brushing	Toluene	154.9 ± 1	96	10	43
Hydroxyl-terminated polydimethylsiloxane, tetraethyl orthosilicate, dibutyltin dilaurate, fumed silica with a specific surface area of 200 ± 25 $m^2 g^{-1}$	Dip coating	*n*-Hexane, paraffin oil, toluene, vegetable oil	156 ± 1	97–99	50	44
Dopamine hydrochloride, tris(hydroxymethyl)aminomethane, stearic acid, copper(II) sulfate pentahydrate, hydrogen peroxide	Dip coating	Trichloromethane	162.0	~100	5	45

superhydrophobic cotton by applying polydopamine (PDA) followed by surface modification using stearic acid. The prepared sample exhibited a WCA of 162° and a sliding angle of 7.8°. The volume of water was measured before and after the oil–water separation and the separation efficiency was found to be ~100%.[45]

Comparative results of recent studies on superhydrophobic cotton fabrics for oil–water separation are given in Table 16.3.

16.3.4 Superhydrophobic Membranes

Moatmed *et al.* prepared a free-standing and flexible nanofibrous superhydrophobic/superoleophilic membrane by electrospinning using Fe_3O_4 NPs embedded in polystyrene nanofibres for oil–water separation. The superhydrophobic membrane exhibited a WCA of 162° and showed a separation efficiency of 99.8% for hexane in a gravity-driven separation. It was reported that the superhydrophobic membrane showed a separation efficiency of 99.8% for low-density oils and 92% for high-density oils.[46] Ma *et al.* first obtained a free-standing polyimide (PI) nanofibrous hydrophilic membrane by the electrospinning technique. The PI membranes were immersed alternately in phytic acid solution and ferric chloride solution multiple times and finally immersed in octadecyltrimethoxysilane solution to obtain a superhydrophobic membrane. The superhydrophobic membrane showed a high efficiency in the separation of various oils, including dichloromethane, trichloromethane, dichloroethane, bromobenzene and carbon tetrachloride, from oil–water mixtures. The membrane maintained a separation efficiency of >99% along with a high separation flux of 8424×10^5 L m^{-2} h^{-1} even after 20 separation cycles.[47]

Wang *et al.* fabricated an ultrathin polytetrafluoroethylene fibrous membrane (UTPFM) using an electro-centrifugal spinning method. A tree-grape-like structure was observed on the membrane fibres. A schematic diagram of the process for the fabrication of the membrane is shown in Figure 16.6a. Figure 16.6b illustrates the growing process of tree grapes. The number and size of the grape structure depend on the concentration of polyvinylpyrrolidone (PVP)–polytetrafluoroethylene (PTFE) (Figure 16.6c). The sample names UTPFM-1, UTPFM-2, UTPFM-3 and UTPFM-4 are related to PVP : PTFE ratios of 1 : 6, 1 : 4, 1 : 2.5 and 1 : 1, respectively. Figure 16.6d–g show SEM images of the membrane with changes in the grape structure for different PVP : PTFE ratios. As the ratio of PVP to PTFE increases, a grape on the fibre surface becomes larger. The average diameter of the grapes varied as 0.6, 0.9, 1.4 and 1.8 μm (Figure 16.6d–g). As the grapes became larger and more numerous, the membrane surface became rougher (Figure 16.6h–k). The optimized PVP–PTFE fibrous membrane showed high porosity along with a WCA of 154.6°. The membrane showed a permeability of 3200 L m^{-2} h^{-1} and a separation efficiency of 99% during gravity-driven separation. The membrane maintained its superhydrophobicity (with a WCA of 153.6°) after 1000 cycles of abrasion.[48]

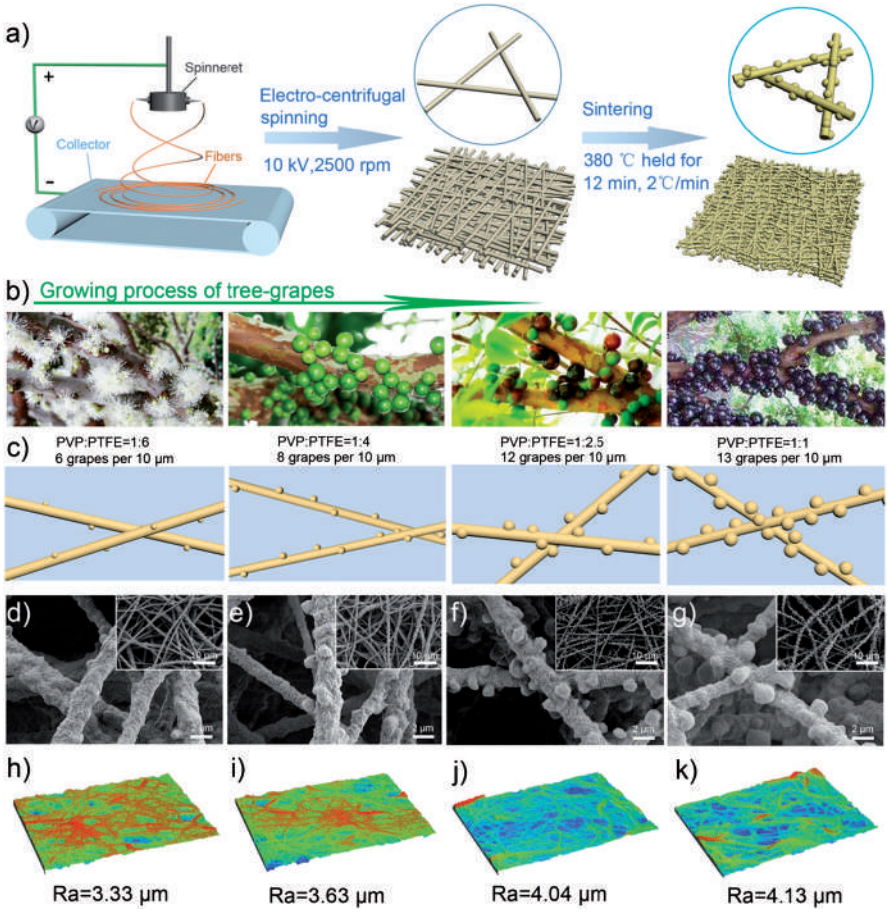

Figure 16.6 (a) Schematic diagram of the fabrication process for UTPFM. (b) Growth of tree grapes. (c) Schematic diagram of the growing process of UTPFMs. SEM images of (d) UTPFM-1, (e) UTPFM-2, (f) UTPFM-3 and (g) UTPFM-4. (h–k) 3D surface morphology and roughness of UTPFMs. Reproduced from ref. 48 with permission from Elsevier, Copyright 2021.

Su *et al.* generated pine-needle-like titanium dioxide (TiO_2) nanorods (TNs) on poly(vinylidene fluoride-*co*-hexafluoropropylene) nanofibre (PNF) membranes *via* a hydrothermal process and then modified them using 1*H*,1*H*,2*H*,2*H*-perfluorodecyltriethoxysilane (PFDS) to obtain a superhydrophobic PNF@TNsPFDS membrane. The PNF membrane was prepared by solution blow spinning (SBS), and its surface morphology is shown in Figure 16.7a. The purpose of SBS is to generate a high-speed airflow to compress and elongate the solution drop, which subsequently solidifies into nanofibres after the solvent has evaporated. The TNs were generated by a two-step

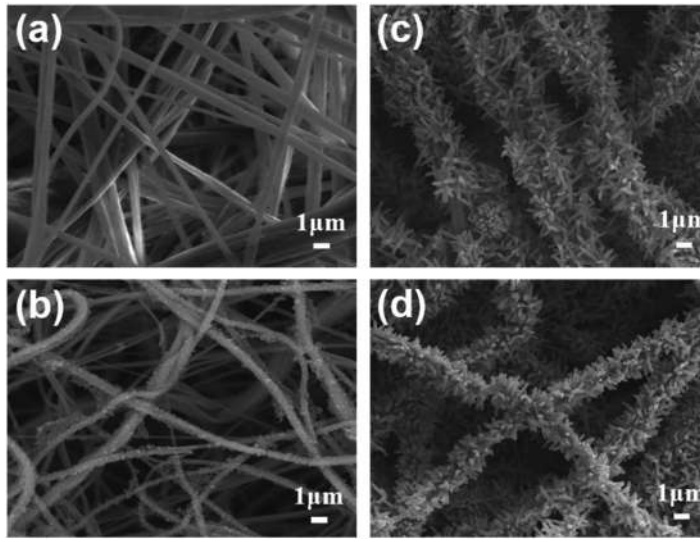

Figure 16.7 SEM images of (a) pristine PNFs, (b and c) growth of TCs and TNs on PNFs, respectively, and (d) PNF@TNsPFDS fibres. Reproduced from ref. 49 with permission from Elsevier, Copyright 2021.

hydrothermal process: in the first step TiO_2 crystals (TCs) were grown and in the second step nanorods (TNs) were formed. The growth of TiO_2 crystals and TNs can be seen in Figure 16.7b and c, respectively. Figure 16.7d indicates that the PFDS modification did not affect the surface structure. The membrane exhibited a WCA of 155.0° and an OCA of 0°. The superhydrophobic membrane showed a separation efficiency of 99.99% for different types of oils such as dichloromethane, *n*-hexane, toluene and kerosene.[49]

Zareei Pour *et al.* fabricated superhydrophobic/superoleophilic electrospun poly(vinylidene fluoride) (PVDF) membranes followed by chemical vapour deposition of dichlorodimethylsilane. The prepared membrane showed high water repellency and breathability and oil sorption and oil–water separation properties. The nanofibrous membranes showed an oil–water separation efficiency of 100.0, 93.7, 23.3, 35.0 and 100.0% for *n*-hexane, kerosene, crude oil, frying oil and toluene–water mixture, respectively.[50]

Comparative results of recent studies on superhydrophobic nanofibrous membranes for oil–water separation are given in Table 16.4.

16.4 Conclusions and Outlook

This chapter has addressed the most recent progress in the fabrication of superhydrophobic/superoleophilic coatings on common substrates, such as meshes, sponges, cotton textiles and membranes, for oil–water separation applications. The most commonly used fabrication techniques for achieving a superhydrophobic surface were briefly discussed. It is concluded that

Table 16.4 Representative reports on superhydrophobic/superoleophilic membranes for oil–water separation.

Materials	Method	Types of oil/organic solvent	WCA/°	Separation efficiency/%	Reusability/ cycles	Ref.
Polystyrene and Fe_3O_4 nano-powder with ~50 nm particle size	Electrospinning	*n*-Hexane, petroleum ether, gasoline oil, olive oil, sesame oil	162	99.8	50	46
Ferric chloride hexahydrate, octadecyltrimethoxysilane, phytic acid, 3,3′,4,4′-biphenyl tetracarboxylic dianhydride, *p*-phenylenediamine	Electrospinning	DCM (dyed with Sudan III for easy observation), trichloromethane, dichloroethane, bromobenzene, carbon tetrachloride	154.73 ± 1.8	99	20	47
PTFE, polyvinylpyrrolidone, poly(vinyl alcohol)	Electro-centrifugal spinning	Water-in-0.65 $mm^2\ s^{-1}$ and water-in-5 $mm^2\ s^{-1}$ silicone oil emulsion	154.6	>99	200	48
Poly(vinylidene fluoride-*co*-hexafluoropropylene), 1*H*,1*H*,2*H*,2*H*-perfluorodecyltriethoxysilane, tetrabutyl titanate	Two-step hydrothermal	Dichloromethane, *n*-hexane, toluene, kerosene	155.0	99.99	10	49
Poly(vinylidene fluoride), dichlorodimethylsilane	Electrospinning technique and chemical vapour deposition	*n*-Hexane, kerosene, crude oil, frying oil, toluene	152.0 ± 2.5	100.0 for toluene	10	50

superhydrophobic/superoleophilic meshes, sponges, cotton textiles and membranes exhibit outstanding oil and water separation from oil–water mixtures and emulsions. Metal mesh is a ductile, porous and durable substrate whereas cotton textiles and membranes are highly flexible and porous and superhydrophobicity could be easily achieved by depositing a functional material because they have pre-existing hierarchical surface structures. Three-dimensional sponges demonstrated a capability for high-volume liquid absorption, hence superhydrophobic/superoleophilic sponges easily remove oil from oil–water mixtures.

Despite the substantial progress made in these areas, there are still some obstacles to be addressed in future research:

1. The hierarchical nano/microstructure is damaged under harsh conditions that affect the wetting properties.
2. Repetition of the oil–water separation process can block the pores of the substrate, consequently reducing the separation efficiency.
3. Functional materials become detached from the substrate during repeated oil–water separation.
4. Fabrication costs should be lowered for large-scale production.
5. Maintaining the surface properties for the separation of low- and high-viscosity oils is challenging.

Acknowledgements

This work was financially supported by the DST – INSPIRE Faculty Scheme, Department of Science and Technology (DST), Government of India (DST/INSPIRE/04/2015/000281).

References

1. R. K. Gupta, G. J. Dunderdale, M. W. England and A. Hozumi, *J. Mater. Chem. A*, 2017, **5**, 16025–16058.
2. S. S. Latthe, C. Terashima, K. Nakata, M. Sakai and A. Fujishima, *J. Mater. Chem. A*, 2014, **2**, 5548–5553.
3. S. Wang, K. Liu, X. Yao and L. Jiang, *Chem. Rev.*, 2015, **115**, 8230–8293.
4. E. Vazirinasab, R. Jafari and G. Momen, *Surf. Coat. Technol.*, 2018, **341**, 40–56.
5. L. Li, B. Li, J. Dong and J. Zhang, *J. Mater. Chem. A*, 2016, **4**, 13677–13725.
6. Z. Liu, H. Wang, X. Zhang, C. Wang, C. Lv and Y. Zhu, *Chem. Eng. J.*, 2017, **326**, 578–586.
7. J.-W. Lee and W. Hwang, *Mater. Lett.*, 2016, **168**, 83–85.
8. M. Xiong, Z. Ren and W. Liu, *Cellulose*, 2019, **26**, 8951–8962.
9. K.-M. Lee, H. Park, J. Kim and D.-M. Chun, *Appl. Surf. Sci.*, 2019, **467**, 979–991.

10. G. Polizos, G. G. Jang, D. B. Smith, F. List, M. G. Lassiter, J. Park and P. G. Datskos, *Sol. Energy Mater. Sol. Cells*, 2018, **176**, 405–410.
11. Z. Chen, L. Hao, A. Chen, Q. Song and C. Chen, *Electrochim. Acta*, 2012, **59**, 168–171.
12. S. Rasouli, N. Rezaei, H. Hamedi, S. Zendehboudi and X. Duan, *Mater. Des.*, 2021, **204**, 109599.
13. J. Xue, T. Wu, Y. Dai and Y. Xia, *Chem. Rev.*, 2019, **119**, 5298–5415.
14. C. Luo, S. D. Stoyanov, E. Stride, E. Pelan and M. Edirisinghe, *Chem. Soc. Rev.*, 2012, **41**, 4708–4735.
15. N. Ashammakhi, I. Wimpenny, L. Nikkola and Y. Yang, *J. Biomed. Nanotechnol.*, 2009, **5**, 1–19.
16. D. Hetemi and J. Pinson, *Chem. Soc. Rev.*, 2017, **46**, 5701–5713.
17. M. A. Aegerter and M. Mennig, *Sol-gel Technologies for Glass Producers and Users*, Springer Science & Business Media, 2013.
18. K. Ariga, Y. Yamauchi, G. Rydzek, Q. Ji, Y. Yonamine, K. C.-W. Wu and J. P. Hill, *Chem. Lett.*, 2014, **43**, 36–68.
19. T. Ogawa, B. Ding, Y. Sone and S. Shiratori, *Nanotechnology*, 2007, **18**, 165607.
20. J. J. Richardson, M. Björnmalm and F. Caruso, *Science*, 2015, **348**, aaa2491.
21. X. Tang and X. Yan, *J. Sol-Gel Sci. Technol.*, 2017, **81**, 378–404.
22. J. Puetz and M. Aegerter, *Sol-gel Technologies for Glass Producers and Users*, 2004, pp. 37–48.
23. H. Kaur, V. K. Bulasara and R. K. Gupta, *Carbohydr. Polym.*, 2018, **195**, 613–621.
24. B. Nandi, R. Uppaluri and M. Purkait, *J. Membr. Sci.*, 2009, **330**, 246–258.
25. M. Tawalbeh, A. Al Mojjly, A. Al-Othman and N. Hilal, *Desalination*, 2018, **447**, 182–202.
26. Z. Hu, J. Zhang, S. Xiong and Y. Zhao, *Org. Electron.*, 2012, **13**, 142–146.
27. F. Aziz and A. F. Ismail, *Mater. Sci. Semicond. Process.*, 2015, **39**, 416–425.
28. A. Makhlouf, in *Nanocoatings and Ultra-thin Films*, Elsevier, 2011, pp. 3–23.
29. T. Darmanin, E. T. de Givenchy, S. Amigoni and F. Guittard, *Adv. Mater.*, 2013, **25**, 1378–1394.
30. I. Gurrappa and L. Binder, *Sci. Technol. Adv. Mater.*, 2008, **9**, 043001.
31. U. Zulfiqar, S. Z. Hussain, T. Subhani and I. Hussain, *Colloids Surf., A*, 2018, **539**, 391–398.
32. H. Chen, Y. Shen, Z. He, Z. Wu and X. Xie, *J. Mater. Sci. Technol.*, 2020, **51**, 151–160.
33. V. Singh, Y.-J. Sheng and H.-K. Tsao, *J. Taiwan Inst. Chem. Eng.*, 2018, **87**, 150–157.
34. B. K. Tudu and A. Kumar, *Prog. Org. Coat.*, 2019, **133**, 316–324.
35. P. Varshney, D. Nanda, M. Satapathy, S. S. Mohapatra and A. Kumar, *New J. Chem.*, 2017, **41**, 7463–7471.
36. E.-C. Cho, C.-W. Chang-Jian, H.-C. Chen, K.-S. Chuang, J.-H. Zheng, Y.-S. Hsiao, K.-C. Lee and J.-H. Huang, *Chem. Eng. J.*, 2017, **314**, 347–357.

37. J. Peng, J. Deng, Y. Quan, C. Yu, H. Wang, Y. Gong, Y. Liu and W. Deng, *ACS Omega*, 2018, **3**, 5222–5228.
38. L. Zou, A. D. Phule, Y. Sun, T. Y. Zhu, S. Wen and Z. X. Zhang, *Polym. Test.*, 2020, **85**, 106451.
39. H. Sun, Z. Liu, K. Liu, M. E. Gibril, F. Kong and S. Wang, *Ind. Crops Prod.*, 2021, **170**, 113798.
40. S. Liu, Q. Zhang, L. Fan, R. Wang, M. Yang and Y. Zhou, *Ind. Eng. Chem. Res.*, 2020, **59**, 11713–11722.
41. Q.-Y. Cheng, X.-L. Zhao, Y.-X. Weng, Y.-D. Li and J.-B. Zeng, *ACS Sustainable Chem. Eng.*, 2019, **7**, 15696–15705.
42. S. Gao, X. Dong, J. Huang, S. Li, Y. Li, Z. Chen and Y. Lai, *Chem. Eng. J.*, 2018, **333**, 621–629.
43. L. Li, J. Zhu and Z. Zeng, *Prog. Org. Coat.*, 2020, **147**, 105863.
44. P. Talebizadehsardari, J. Seyfi, I. Hejazi, A. Eyvazian, M. Khodaie, S. Seifi, S. M. Davachi and H. Bahmanpour, *Colloids Surf., A*, 2020, **603**, 125204.
45. X. Dong, S. Gao, J. Huang, S. Li, T. Zhu, Y. Cheng, Y. Zhao, Z. Chen and Y. Lai, *J. Mater. Chem. A*, 2019, **7**, 2122–2128.
46. S. M. Moatmed, M. H. Khedr, S. El-Dek, H.-Y. Kim and A. G. El-Deen, *J. Environ. Chem. Eng.*, 2019, **7**, 103508.
47. W. Ma, M. Zhang, Z. Liu, C. Huang and G. Fu, *Environ. Sci.: Nano*, 2018, **5**, 2909–2920.
48. A. Wang, X. Li, T. Hou, Y. Lu, J. Zhou, X. Zhang and B. Yang, *Sep. Purif. Technol.*, 2021, **275**, 119165.
49. Y. Su, T. Fan, H. Bai, H. Guan, X. Ning, M. Yu and Y. Long, *Sep. Purif. Technol.*, 2021, **274**, 119098.
50. F. Zareei Pour, M. M. Sabzehmeidani, H. Karimi, V. M. Avargani and M. Ghaedi, *J. Appl. Polym. Sci.*, 2019, **136**, 47621.